IDENTIFICATION OF OPTIMAL RENDEZVOUS AND SEPARATION AREAS FOR FORMATION FLIGHT UNDER CONSIDERATION OF WIND

Tobias Marks* , **Majed Swaid**** , **Benjamin Lührs**** , **Volker Gollnick***
***German Aerospace Center** , ****Technical University Hamburg**

Keywords: *formation flight, fuel savings, wind influence*

Abstract

The paper analyzes the influence of wind on the optimal rendezvous and separation points of a two-aircraft aerodynamic formation flight. For a set of origin and destination airports the optimal formation routing is determined for each day of the year 2012 *using an optimal control approach and a pattern search optimization to maximize the benefits estimated by a surrogate model. The resulting formation geometries are recalculated to enhance the benefit estimation and subsequently compared to the cases with fixed rendezvous and separation locations. It is shown, that wind effects account for a large variability of the achievable benefits as well as of the geographic location of the optimal rendezvous and separation points. A fixation of these locations leads to a significant reduction of the achievable benefits.*

1 General Introduction

The formation flight of birds is a fascinating natural phenomenon and a transfer of this principle to man-made aircraft promises substantial fuel savings that can lead to a reduction of not only emissions but also cost. Numerous aerodynamic analyses and flight experiments were conducted throughout the years and it could be shown, that the aerodynamic formation flight (also called wake-surfing) is practicable. Beside the technical aspects of building up a formation, the integration of the new concept into the air transport system poses many challenges as inefficiencies arising from detours, the necessity of speed and altitude adaptions, different aircraft types, timing and delays and not least wind effects influence the achievable fuel savings. The wind effects can be assumed to have a considerable effect on the optimal formation geometry and therefore on the optimal rendezvous and separation points as they essentially affect the formation routing. Hence, this paper will present a method to identify optimal rendezvous and separation areas for a given set of origin and destination airports that yield the highest average benefits under consideration of different wind situations.

1.1 State of the Art

The analysis of operational aspects arising from flying in formation was subject of several works wherein the route optimization and partner allocation problem was of particular importance. Kent et al. [5] showed, that a fast creation of optimal formation routes can be achieved by using a geometric approach. They demonstrated that up to 8.6% fuel savings can be achieved for a transatlantic scenario by two-aircraft formations. Xu et al. [10] showed in another analysis for a North Atlantic scenario, that for an airline network fuel savings of up to 6.8% can be achieved by introducing formation flight. Previous related works by the author deal with the parametrization of formations [7] and the deduction of surrogate models for the benefit estimation [8] and are the basis for the presented work.

1.2 Approach

In this section the general approach of the study presented will be described (see figure 1). In the first step of the analysis the scope including the definition of the double origin/destination pairs (DODPs) is defined (see chapter 2). A DODP describes a two-aircraft formation mission and defines the origin and destination airports of the leader and follower aircraft accordingly. Once the DODP is defined, optimal formation geometries (FG) including the rendezvous and separation points (rendezvous start point; RSP, separation end point; SEP) will be identified using an optimal control approach as described in chapter 3.1. The calculations will be performed under the consideration of wind effects for the time period of a whole year. The

RSP and SEP locations will be used subsequently to determine average RSP and SEP locations along with the resulting FGs (see chapter 3.2). All FGs will be recomputed by a trajectory calculation (see chapter 3.3) and finally be evaluated.

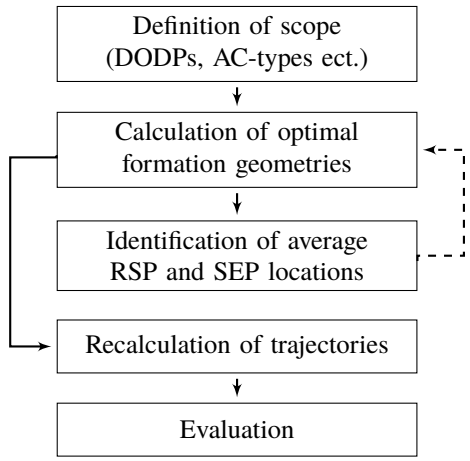

Fig. 1 : General approach.

2 Scope

To conduct the presented study, several assumptions need to be taken and boundary conditions are to be set which will be described in this section. Formation flight can be performed with a variable number of members participating in one formation. As it can be assumed that the two-aircraft formation will be the first to be realized, this paper focuses on two-aircraft formations only. Furthermore, it will be assumed, that both formation members are of the same aircraft type which was selected to be the Boeing 777-200 as one of the most prevalent aircraft used on the North Atlantic. The passenger loadfactors of both aircraft are fixed to 0.8 in accordance with IATA [3]. The formation cruise altitude (FCA) and the formation cruise Mach number (FCM) are fixed to $FCA = 39000ft$ and $FCM = 0.84$ representing the standard cruise speed of the B777-200. In order to construct a formation geometry (FG) the origin and destination airports of the formation members need to be known. This so called double OD-pair (DODP) was selected by analyzing flightplan data of transatlantic flights in westbound direction. The two most frequented connections were identified to be LHR-JFK and CDG-YUL, which were selected as the main DODP accordingly. For the variation of the follower airport other major European airports (AMS, FRA, and HAM) were chosen to guarantee adequate spatial variation. In order to distinguish the DODPs, only the follower origin airport will be used, as all other airports remain the same. Table 1 summarizes the scope of the study.

AC-type	Boeing 777-200
FCA	39000ft
FCM	0.84
loadfactor	0.8
ld Origin	LHR
ld Destination	JFK
fw Origin	AMS, CDG, FRA, HAM
fw Destination	YUL
year	2012
days	366

Tab. 1 : Scope of the study.

2.1 Cases

Within this paper several case studies will be analyzed (see table 2). In the initial case all wind optimal RSP/SEP combinations for all DODPs will be calculated for each day of the year 2012. This case is called the *opt* case.

case	**index**	**RSP/SEP**
no wind	nwd	optimal without wind
optimal	opt	optimal with wind
direct	dct	fixed per DODP
direct all	all	fixed for all

Tab. 2 : Examined cases.

The direct or *dct* case describes the routing of all formations of a distinct DODP over a common RSP/SEP combination for the particular DODP under consideration. The *all* case describes the case that all fomations of all DODPs are routed over one single common RSP/SEP combination. For reference the *nwd* case describes the case that no wind influence occurs and the segments of the FG therefore equal great circle segments. The construction of the geometrically optimal RSP/SEP combination according to [5] is not applicable in the presented case as shown by [1] and can, therefore, not be evaluated for comparison.

2.2 Meteorological Data

The underlying data for the windoptimal calculation is extracted from the European reanalysis interim data set (ERA) provided by the European center for medium range weather forecast (ECMWF; [2]). The therein contained reanalysis data is arranged in a coordinate grid with a resolution of 0.75 ° in both latitude and

longitude. The vertical resolution is given by 60 layers between the surface and a pressure altitude level of 0.1 hPa. The data contains information on temperature, pressure, relative humidity and wind speeds in eastward- and northward direction. For the evaluation the data at 12 UTC on a particular day was used.

3 Methods

3.1 Calculation of optimal RSP and SEP

Figure 2 shows the approach used to derive a wind optimal FG. In the first step for a given RSP/SEP combination wind optimal route segments are calculated using the route optimization technique as desribed in chapter 3.1.1. In this process it is checked, wheather the top of climb (ToC) and top of descent (ToC) locations are suitable (see chapter 3.1.5). The single segments are then assembled to form a FG (see chapter 3.1.2). The achievable benefit of this FG is subsequently assessed using surrogate models as described in chapter 3.1.3. An overall optimization process then varies the RSP/SEP combination in order to determine the optimal FG using a pattern search algorithm (see chapter 3.1.4).

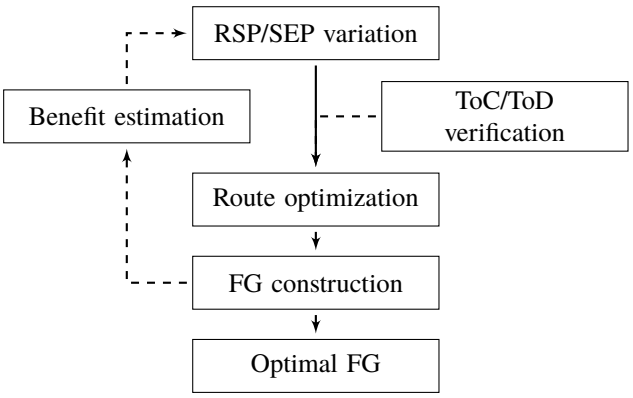

Fig. 2 : Calculation of an optimal formation geometry.

3.1.1 Route optimization

Within this study, minimum time tracks during cruise-flight in the horizontal plane are estimated based on an optimal control approach. Therefore, the aircraft is assumed to be a massless point, moving along a spherical earth (radius R_E) with a constant true airspeed v_{TAS} at a constant pressure altitude H_p with both values being derived from the specified FCA and FCM of the formation using the international standard atmosphere (ISA). The flight direction can be affected by changing the heading angle χ_H which serves as control variable.

$$\dot{\lambda} = \frac{v_{\mathrm{TAS}} \sin\chi_{\mathrm{H}} + u_{\mathrm{W}}(\lambda,\varphi)}{R_{\mathrm{E}} \cos\varphi} \tag{1}$$

$$\dot{\varphi} = \frac{v_{\mathrm{TAS}} \cos\chi_{\mathrm{H}} + v_{\mathrm{W}}(\lambda,\varphi)}{R_{\mathrm{E}}} \tag{2}$$

$$J = \int_{t_0}^{t_f} 1\,dt \tag{3}$$

Additionally, the surrounding wind and pressure conditions are expected to be stationary. Presuming the flight path angle γ to be very small (H_p is constant) and $H_p \ll R_E$, the aircraft's equations of motion - constituting the dynamic constraints of the optimal control problem - can be formulated (see eq. 1 and 2). Here, λ represents the longitude, φ the latitude, u_W the wind speed in eastward direction and v_W the wind speed in northward direction. The cost functional J of the optimal control problem is chosen to be the flight time between the initial position 0 to the final position f according to eq. 3. Finally, the optimal control problem is defined as identification of the temporal evolution of the heading angle χ_H which minimizes the flight time according to eq. 3 while satisfying the dynamic constraints defined by eq. 1 and 2. This formulation represents Zermelo's problem on a spherical earth [11]. Applying Pontryagin's minimum principle [9] to the resulting optimal control problem, yields the optimal control law for the heading angle χ_H as shown in eq. 4. A detailed derivation of eq. 4 is given by Lührs et al. [6].

$$\begin{aligned}\dot{\chi}_{\mathrm{H}} = &\frac{\partial u_{\mathrm{W}}}{\partial\varphi}\frac{\sin^2\chi_{\mathrm{H}}}{R_{\mathrm{E}}} - \frac{\partial v_{\mathrm{W}}}{\partial\lambda}\frac{\cos^2\chi_{\mathrm{H}}}{R_{\mathrm{E}}\cos\varphi} \\ &+ \left(\frac{\partial v_{\mathrm{W}}}{\partial\varphi} - \frac{\partial u_{\mathrm{W}}}{\partial\lambda}\frac{1}{\cos\varphi}\right)\frac{\sin\chi_{\mathrm{H}}\cos\chi_{\mathrm{H}}}{R_{\mathrm{E}}} \\ &+ \frac{\tan\varphi\sin\chi_{\mathrm{H}}}{R_{\mathrm{E}}}\left(v_{\mathrm{TAS}} + u_{\mathrm{W}}\sin\chi_{\mathrm{H}} + v_{\mathrm{W}}\cos\chi_{\mathrm{H}}\right)\end{aligned} \tag{4}$$

The system of differential equations 1, 2 and 4 is integrated by using a shooting method in order to solve a two point boundary value problem with given initial and final values of latitude and longitude or for a given initial position and various initial headings.

3.1.2 Construction of a formation geometry

The route optimization method described in chapter 3.1.1 is used to construct a formation geometry according to [8] that consists of several parts that are shown in figure 3 and listed below.

- Reference tracks (index *ref*)
- Approach segments (index *a*)
- Formation segment (index *ben*)
- Continuation segments (index *b*)

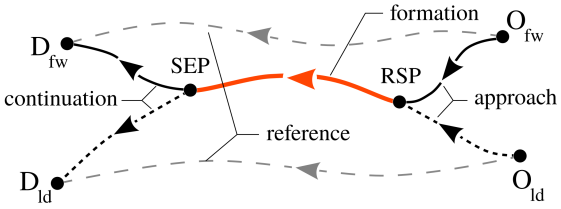

Fig. 3 : Schematic formation geometry (O=origin; D=destination).

Except for the formation segment all other segments as well as the reference tracks need to be determined both for the leader (index *ld*) and for the follower (index *fw*). The route optimization is therefore applied for all single segments of the FG summing up to 7 optimization runs. The results are subsequently combined to form a single FG that can then be used to estimate the formation benefits. Figure 14 shows exemplary FGs calculated by the method described above. It can clearly be seen, that due to the wind influence the optimal FGs strongly differ from the great circle routes.

3.1.3 *Benefit estimation*

For the purpose of describing the benefits obtained by a formation, the relative formation efficiency metric λ_F is used (see eq. 5). λ_F describes the absolute fuel savings ΔF_F in relation to the fuel necessary for the reference missions F_{Fref}. The fuel savings ΔF_F is the difference of F_{Fref} and the fuel necessary for the formation mission F_{Fform}. Hence, a positive λ_F means, that the formation will save fuel.

$$\lambda_F = \frac{\Delta F_F}{F_{Fref}} = \frac{F_{Fref} - F_{Fform}}{F_{Fref}} = \frac{\sum F_{ref} - \sum F_{form}}{\sum F_{ref}} \quad (5)$$

The benefit estimation of a FG is based on surrogate models. As shown in [8] surrogate models for the relative formation efficiency metric λ_F can be derived based on a set of geometric and mission data. Therefore, λ_F can be expressed as a function of 11 parameters (see equation 6). These parameters include the relative detours (σ), the relative segment lengths of the approach (ξ_a) and the formation segment (ξ_{ben}) (see eq. 7) as well as a scaling length (S).

$$\lambda_F, \Delta F_F = f(\sigma_{ld}, \sigma_{fw}, \xi_{ben\,ld}, \xi_{ben\,fw}, \xi_{a\,ld}, \xi_{a\,fw}, FCM, FCA, lf_{ld}, lf_{fw}, S_{route\,ld}) \quad (6)$$

For the B777-200/B777-200 pairing an analogous kriging model was used that was derived by a set of exemplary trajectory calculations taking into account the aerodynamic benefit of the follower using the trajectory calculation method as described in chapter 3.3.

$$\xi_a = \frac{S_a}{S_{route}} \qquad \xi_{ben} = \frac{S_{ben}}{S_{route}} \qquad \sigma = \frac{S_{route} - S_{ref}}{S_{ref}} \quad (7)$$

For a given FG the necessary formation parameters can easily be derived. However, as the surrogate models are calculated for the case without wind influence using ground distances as a baseline, the parameters in the wind case have to be calculated based on the according air distances to take into account the wind effects.

3.1.4 *RSP/SEP optimization*

The achievable benefits vary with the location of the RSP and SEP and show a distinct maximum (see also chapter 4.1) allowing the use of regular optimization techniques. Therefore, in order to find the optimal locations of the RSP and SEP for a given windfield, a pattern search algorithm was developed. Figure 4 shows an example of this algorithm optimizing the RSP/SEP combination (only RSP part shown). The algorithm samples possible RSP/SEP combinations on a grid centered around a starting combination. The size of the grid was chosen to be 3 by 3 with a 2.5 ° spacing. For these resulting 81 RSP/SEP combinations windoptimal FGs are calculated as described in chapter 3.1.2 and the benefit is estimated using the surrogate model for λ_F (blue points). If a better solution than in the previous steps is found, it will be chosen as the new starting combination for the next iteration of the algorithm (red arrows). If no better solution could be determined, the size of the grid is halved (green arrows). By this process the location of the maximum benefit is narrowed down. For the initial points RSP_{start} and SEP_{start} a point between the reference tracks is chosen. Furthermore, the alogrithm takes into account, that formation flight can only be established in cruise flight. Therefore, the ToC and ToD for the calculated track using the RSP/SEP combination are estimated as described in chapter 3.1.5. If the RSP and SEP under evaluation cannot be used due to an unfulfilled ToD or ToC constraint, the algorithm will not investigate this

solution any more (black points). In order to accelerate the algorithm, a pointlist is used that holds the already sampled RSP/SEP combinations for fast lookup. If the spacing of the grid falls below 0.078125 °, the stop criterion for the algorithm is reached. The RSP/SEP location with the highest λ_F will be considered the optimal RSP_{opt} and SEP_{opt}.

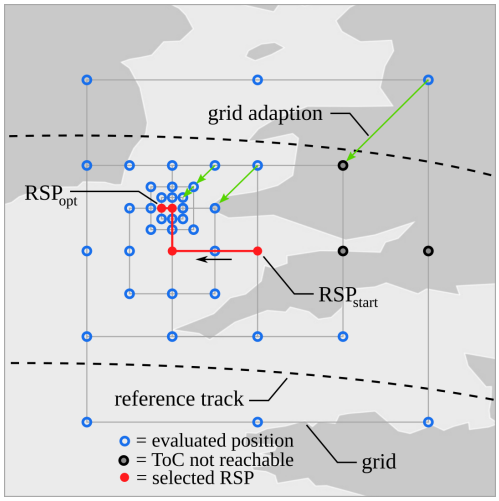

Fig. 4 : Example for the pattern search algorithm (RSP location only). The same method is used to optimize the SEP location simultaneously.

3.1.5 ToC/ToD calculation

In order to estimate the location of the ToC and ToD in the case of wind consideration, a mapping method was used. This method maps the climb and descent trajectories of a standard profile (case with no wind influence) to the optimal route derived by the route optimization taking into account the wind situation. This process is shown in figure 5.

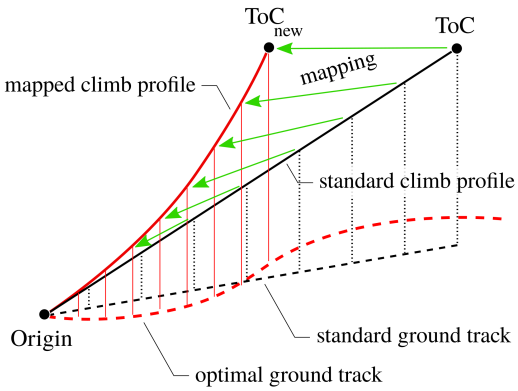

Fig. 5 : Schematic mapping process to estimate the ToC of a wind optimal route.

For each timestep the position of the aircraft along the optimal ground track is estimated, while the local wind velocity is interpolated at the given position and superimposed over the aircraft speed derived from the standard climb profile. Applying this procedure, a mapped climb profile is constructed and the ToC can be derived. This method can also be used to determine the descent profile and the ToD accordingly.

3.2 Determination of common RSP and SEP

In order to determine the optimal rendezvous and separation areas, the average RSP and SEP locations are determined. This is done by estimating the density δ of the points using radial base functions (RBF) with an underlying spherical metric. For the kernel of the RBF the weighted gauss function

$$k(d, \lambda_F) = \exp\left(-\frac{1}{r} \cdot d^2\right) \cdot \lambda_F \tag{8}$$

is chosen with d as the great circle distance from the origin. The influence r of the points was chosen to be 0.5 ° in accordance with the resolution of the optimization. The density δ_j at a point P_j can then be calculated by using eq. 8 and is given by

$$\delta_j = \sum_i \exp\left(-\frac{1}{r} \cdot d_{ij}^2\right) \cdot \lambda_{Fi} \tag{9}$$

The positions δ_{max} with the highest densities are considered to be candidates for a common RSP and SEP and will be called RSP_{dct} and SEP_{dct} in the *dct* case and RSP_{all} and SEP_{all} in the *all* case. Furthermore, the variation V of the optimal RPSs and SEPs can be evaluated by the average pairwise great circle distances between two points that can be calculated by

$$V = \frac{1}{n^2} \sum_{i=1}^{n} \sum_{j=1}^{n} d_{ij}^2 \tag{10}$$

with d_{ij} representing the great circle distances between a pair of points P_i and P_j.

3.3 Recalculation of trajectories

For the recalculation of the FGs, an adapted version of the trajectory calculation module (TCM) was used that calculates the formation flight benefits under consideration of wind. TCM uses the base of aircraft data (BADA) flight performance models version 4 provided by Eurocontrol. The formation flight benefits are modeled by calculating the average upwash at the follower

position created by two hallock burnham vortices generated by the leader and superposition of this upwash to the followers speed. For further details on the calculation method refer to [7].

4 Results

In this chapter the results of the studies will be presented. First, the contours of the benefits will be presented followed by an analysis of the RSP/SEP locations. After a short statistical overview, the benefits will be analyzed on a daily, monthly and yearly basis.

4.1 Formation efficiency contours

The benefits that are achievable by a formation vary with the locations of the RSP and the SEP. Figure 6 shows the resulting $\lambda_F = const$ levels as contour plots for the case without wind (black) and the windfield of 5th of January 2012 for the DODP CDG for the RSP location and the SEP location. The calculations were performed using the method described in chapter 3.1 and by a varying the RSP location while fixing the SEP location at the same time and vice versa. For the fixed RSP and SEP locations the optimal locations of the *nwd* case (see table 3) were used. It can be seen, that the wind strongly influences the contours of the achievable benefits and thereby the location and magnitude of the maximum benefit. The contours, however, show a distinct maximum. Therefore, regular optimization techniques (e.g. pattern search as shown in chapter 3.1.4) can be applied in order to localize this maximum.

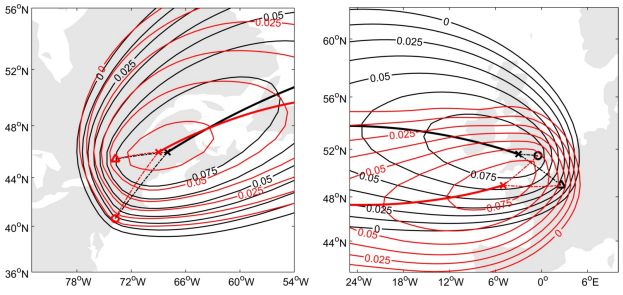

Fig. 6 : λ_F contours for the DODP CDG; no wind (black), wind field of 5th of January (red); SEP variation (left), RSP variation (right).

4.2 RSP/SEP distributions

Figure 7 shows the wind optimal RSP locations for the DODPs under consideration. The colour and the size of the points indicate the magnitude of λ_F. It can be observed, that the optimal positions and the λ_F values strongly vary with the wind situation. The extent reaches basically from Wales and the Celtic Sea over the Irish Sea up to Northern Ireland and Scotland.

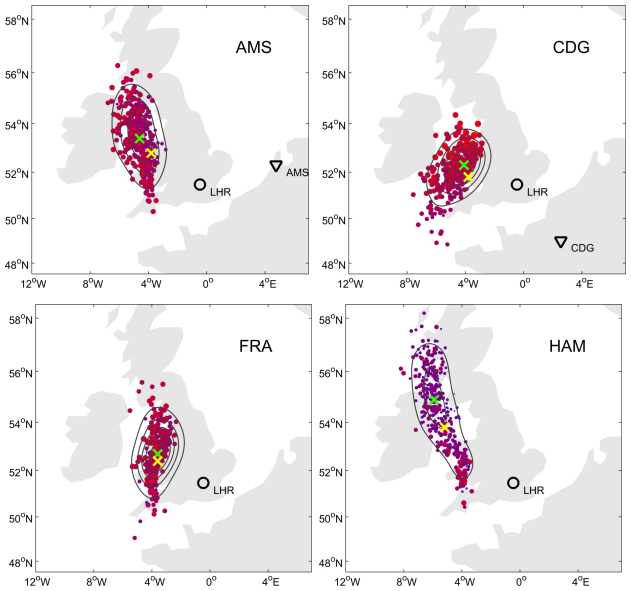

Fig. 7 : Locations and density contours of the wind optimal RSPs separated by DODP; average RSP of *dct* case (green), *nwd* case (yellow).

Furthermore, the observed spread of the RSP locations strongly varies with the DODP. While CDG and FRA show a more compact pattern, the scatter of the RSP locations for AMS and HAM is much higher. This result can also be found in table 4 that shows the variations V of the formation points. The densities show distinct maxima (green). The optimal RSPs in the *nwd* case generally differ from these maxima.

case	DODP	RSP		SEP	
		lat	lon	lat	lon
nwd	AMS	52.8	-3.8	46.7	-67.4
	CDG	51.8	-3.8	46.8	-70.0
	FRA	52.4	-3.6	46.6	-67.6
	HAM	53.8	-5.2	46.5	-68.4
dct	AMS	52.9	-4.4	47.1	-70.0
	CDG	52.2	-4.2	47.2	-68.9
	FRA	52.5	-3.7	47.0	-69.5
	HAM	54.4	-5.7	46.8	-70.7
all		52.5	-3.9	47.0	-69.9

Tab. 3 : Coordinates of the common RSP and SEP positions for the *nwd*, *dct* and *all* case.

The graphs in figure 8 show the wind optimal SEP locations for the DODPs under consideration. The SEP

locations vary from Nova Scotia to Quebec. However, the extent of the SEP locations appears to be generally more consistent regarding the geographical variation of the DODP than in the RSP case. The maximum densities (green) and the optimal SEP locations of the *nwd* case (yellow) also differ more strongly.

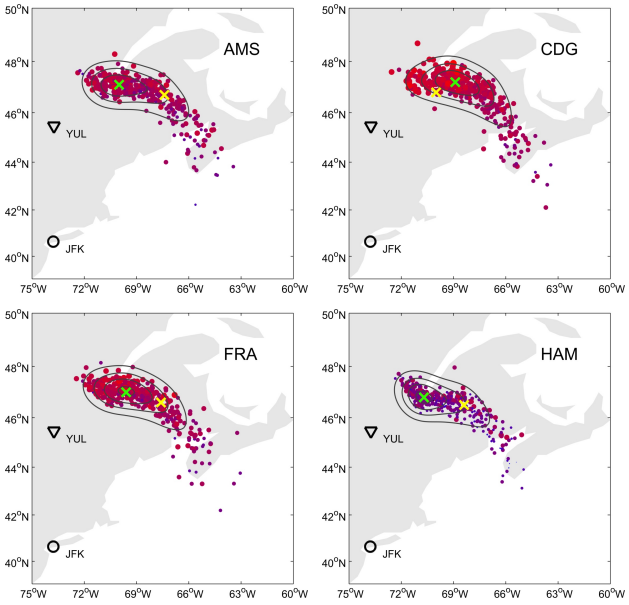

Fig. 8 : Locations and density contours of the wind optimal SEPs separated by DODP; average SEP of *dct* case (green), *nwd* case (yellow).

Figure 9 shows all wind optimal RSP and SEP locations together with the combined RSP and SEP density contours and the locations of the maximum densities (*all* case, see chapter 2, green). It can be found, that the densities show distinct maxima (green) that are not congruent with the maxima for the single DODPs (yellow).

DODP	RSP	SEP
CDG	1.1959	1.8043
AMS	1.4059	1.7763
FRA	1.1371	1.7338
HAM	1.9858	1.5684

Tab. 4 : Variations V of the RSP and SEP locations.

The variations V of the RSP and SEP locations as calculated by equation 10 are shown in Table 4 and cleary show, that the variation of the RSP location is changing strongly with the DODP whereas the variation of the SEP location is more stable.

All resulting coordinates of the common RSP and SEP locations are summarized in table 3.

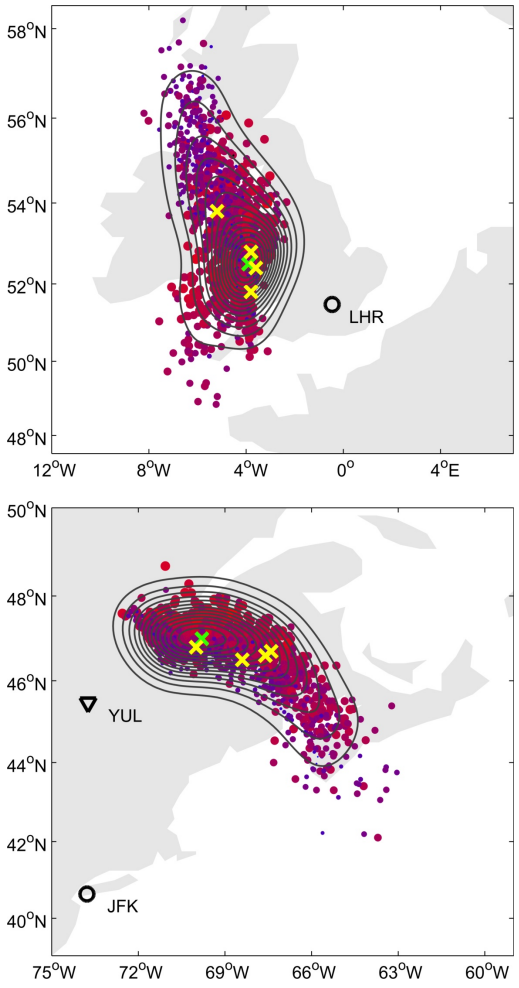

Fig. 9 : Locations and density contours of the wind optimal RSPs and SEPs for all DODPs; average RSP/SEP of *all* case (green) and *dct* cases (yellow).

4.3 Statistical overview

In this chapter a short overview on the statistics of the recalculations will be given. Due to uncertainties in the surrogate model for the estimation of λ_F, that is used by the optimization algorithm described in chapter 3.1.4, a deviation $\Delta\lambda_F$ of the recalculated benefits λ_{Frec} from the estimated benefits λ_{Fsgt} occurs (see eq. 11). Figure 10 (a) shows this deviation over the values estimated by the surrogate model for all DODPs and cases. It can be found, that the deviation is in most cases less that 10% and normally distributed indicating a good accuracy of the surrogate model.

$$\Delta\lambda_F = \frac{\lambda_{Frec} - \lambda_{Fsgt}}{\lambda_{Fsgt}} \tag{11}$$

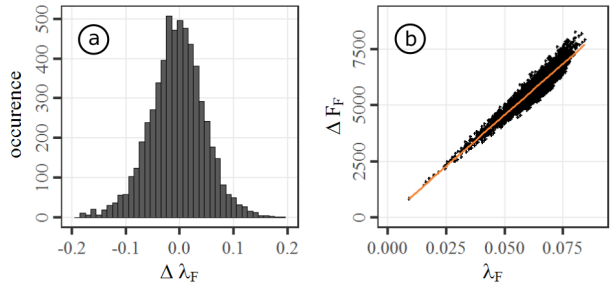

Fig. 10 : Deviation of λ_F between recalculation and surrogate model $\Delta\lambda_F$ (a) and correlation between ΔF_F and λ_F (b).

Figure 10 (b) shows the high correlation (r=0.96) between λ_F and ΔF_F for all calculated missions. Therefore, the relative efficiency metric λ_F will be used for further evaluation of the benefits.

4.4 Examination by day and month

In this chapter the metrics and parameters will be analyzed on both a daily and a monthly basis by means of the DODP AMS.

Benefits

The analysis of the formation flight benefits is essential for the determination of the formation flight potential.

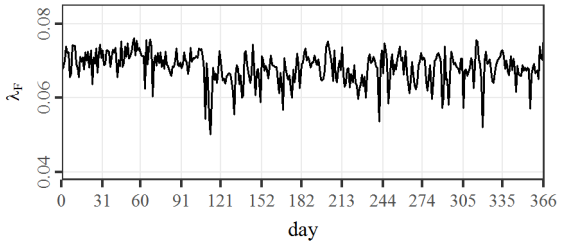

Fig. 11 : Distribution of λ_F for the DODP AMS and the *opt* case over the day.

Figure 11 shows the daily values of λ_F over the course of the year under examination. It can be observed, that the benefits strongly vary over the days between 5% and 8%. Furthermore, it can be seen, that in the middle of the year a slightly increased variance of λ_F occurs compared to the winter months. Figure 12 (a) shows a boxplot of the distributions of the benefits λ_F separated by month. In this figure the change of the variance of λ_F is more evident. The minimum mean benefits occur in the month of May, the maximum mean benefits in February. The winter months generally seem to favor higher benefits.

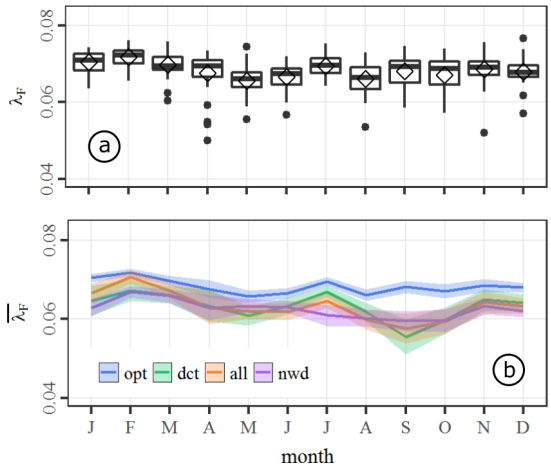

Fig. 12 : Distributions of $\overline{\lambda_F}$ for the DODP AMS and the *opt* case separated by month (a) as well as the monthly means for all cases (b).

Figure 12 (b) shows the mean values of λ_F and all considered cases over the year separated by month. It can be seen, that the mean benefits are strongly reduced in the *dct* and *all* cases. In the *dct* and *all* cases the seasonal effect observed in the *opt* case is even more distinct. This can be explained by the phenomenon that the use of a common RSP/SEP combination curbs the flexibility of the formations to avoid windfields with strong headwinds. This results in higher detours for all formation members, which finally lead to less benefit.

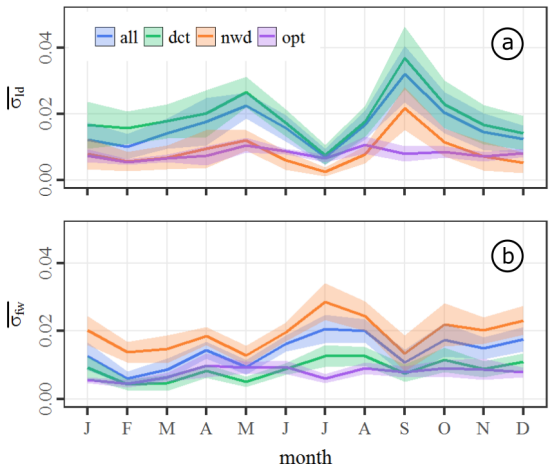

Fig. 13 : Monthly means $\overline{\sigma}$ for the DODP AMS and for all cases separated by leader (a) and follower (b).

Detours

If the detours of the formations from the original routes σ are considered, it can be observed, that they show

the opposite pattern (see figure 13) than the benefits in figure 12. Large detours result in reduced fuel savings, as the detours among other factors can be assumed to significantly influence the benefits. The seasonal pattern can be observed in all considered cases. The highest average detours for the leader occur in the months of May and September for the follower in July and October. The average detours range from 0% up to 4% per month and strongly vary with the case. The leaders show slightly higher detours than the followers. This fact can be attributed to changes in the location of the jetstream, that shifts north and south with the seasons. As the jetstream shifts south in winter, the westbound optimal routes will be located more often north of the jetstream (see [4]). Figure 14 (a) shows the acccording wind optimal tracks on 21st of February 2012. If the jetstream moves north in summer, the optimal routes can be more often be located south of the jetstream. In a formation usually one or both of the members need to take a detour in order to participate. This can lead to the typical splitted situation as it is shown in figure 14 (b) for the 16th of September 2012. Here the reference track of the leader is south, the formation track north of the jetstream, resulting in large detours and thus reduced benefits.

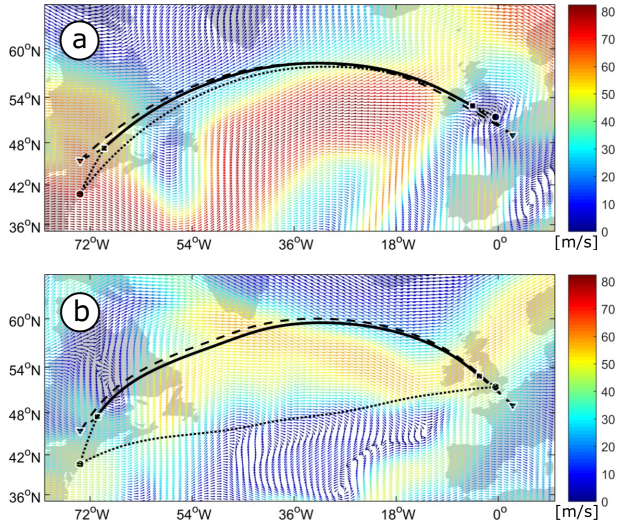

Fig. 14 : Exemplary formation geometries of 21st of February 2012 (a) and 16th of September 2012 (b).

4.5 Examination by year

In this chapter the metrics and parameters will be analyzed on a yearly basis. Figure 15 (a) shows the average yearly relative and absolute benefits of the single DODPs for the considered cases. It can be seen, that the benefits decrease as the RSP location is shifted from the optimal to the common RSP in the *dct* and even more in the *all* case. This decrease accounts for about 0.5% for the DODP CDG and 0.9% for HAM. Furthermore, the DODP HAM shows the least and CDG the highest average benefits. The absolute benefits account for about 4700 kg and 6700 kg of fuel.

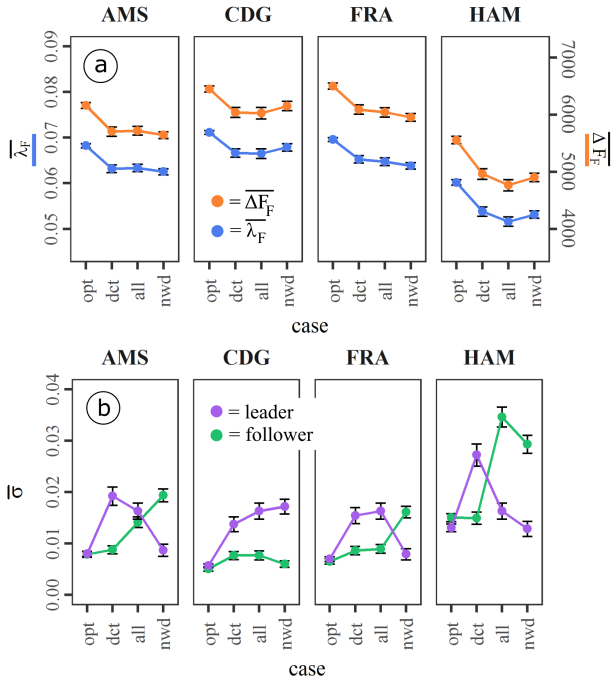

Fig. 15 : Average yearly benefits $\overline{\lambda_F}$ and $\overline{\Delta F_F}$ for all DODPs separated by case (a); average yearly detours $\overline{\sigma}$ for all DODPs separated by case and position (b).

Considering the *nwd* case the DODP CDG and HAM show even higher average benefits than in the *all* and even in the *dct* case, indicating, that the position of the average RSP was not optimal. These findings go along with the average increase of detours as shown in figure 15 (b). The mean detours range from about 0.005% up to 0.027%. It can be seen, that in some cases the order of the maximum mean detours change from leader to follower indicating splitted situations.

5 Conclusions and outlook

Within this work, methods were described, that allow the determination of wind optimal formation geometries, geographic RSP and SEP locations, as well as the estimation of the resulting benefits. It was shown, that a strong variation of the optimal RSP and SEP locations caused by wind effects occurs. The daily benefits, that are achievable during a year, spread over a large range for the considered routes and show in the

year under consideration seasonal changes that might be caused by the shift of the jetstream. The mean relative benefits range from 5% to more than 7% depending on the DODP under consideration representing an average of about 4700 kg to 6700 kg of saved fuel.Furthermore, it was shown, that a fixed RSP/SEP combination for a particular DODP, as well as for all DODPs together, can be determined by a density estimation. However, the use of fixed locations lead to a considerable decrease in the potential relative benefits up to about 1% or 1000 kg of fuel. The more the flexibility of the formation to adapt to the daily wind situation is curbed, the higher the detours will be and the less benefits can be achieved.The common RSP and SEP locations differ strongly from the locations of the case without wind consideration. However, the latter might in some cases lead to higher benefits than the average locations depending on the DODP.
The results suggest, that wind effects cannot be neglected when determining formation flight routing. However, uncertainties in the modeling, especially the aerodynamic model and the determination method of the average RSP and SEP locations are subject to improvement. Also the variation ot flighttimes to the changing RSP locations needs to be taken into account for further studies.

References

[1] Drews, Karim, Marks, Tobias, Konieczny, G., Linke, Florian, and Gollnick, Volker. “Identification and modeling of civil formation flight routes based on global flight schedule data”. In: *66. Deutscher Luft- und Raumfahrtkongress*. 2017.

[2] ECMWF, European Center for Medium range Weather Forecast. URL: https://www.ecmwf.int/.

[3] IATA, International Air Transport Association. *Air Passenger Market Analysis*. 2017.

[4] Irvine, Emma A., Hoskins, Brian J., Shine, Keith P., Lunnon, Robert W., and Froemming, Christine. “Characterizing North Atlantic weather patterns for climate-optimal aircraft routing”. In: *METEOROLOGICAL APPLICATIONS* 20 (2013), pp. 80–93.

[5] Kent, Tom E. and Richards, Arthur G. “Analytic approach to optimal routing for commercial formation flight”. In: *Journal of Guidance, Control, and Dynamics* (Mar. 2015), pp. 1–13. ISSN: 0731-5090.

[6] Lührs, Benjamin, Linke, Florian, and Gollnick, Volker. “Erweiterung eines Trajektorienrechners zur Nutzung meteorologischer Daten für die Optimierung von Flugzeugtrajektorien.” In: *63. Deutscher Luft- und Raumfahrtkongress*. 2014.

[7] Marks, Tobias, Linke, Florian, and Gollnick, Volker. “Ein Ansatz zur Bewertung des Konzeptes von Formationsflügen ziviler Verkehrsflugzeuge im Lufttransportsystem”. In: *62. Deutscher Luft- und Raumfahrtkongress*. 2013.

[8] Marks, Tobias, Linke, Florian, and Gollnick, Volker. “Entwicklung einer Methode zur vereinfachten Ermittlung von Leistungsmerkmalen ziviler Formationsflüge”. In: *63. Deutscher Luft- und Raumfahrtkongress*. 2014.

[9] Pontryagin, L.S., Boltjanskij, V.G., Gamkrelidze, R.V., and Miscenko, E.F. *Mathematische Theorie optimaler Prozesse*. Oldenbourg München, 1967.

[10] Xu, Jia, Ning, S. Andrew, Bower, Geoffrey, and Kroo, Ilan. “Aircraft Route Optimization for Heterogenous Formation Flight”. In: *53rd AIAA Conference*. AIAA 2012-1524. 2012.

[11] Zermelo, Ernst. “Über das Navigationsproblem bei ruhender oder veränderlicher Windverteilung”. In: *Zeitschrift für Angewandte Mathematik und Mechanik* 11 (1931).

6 Contact Author Email Address

tobias.marks@dlr.de

Copyright Statement

The authors confirm that they, and/or their company or organization, hold copyright on all of the original material included in this paper. The authors also confirm that they have obtained permission, from the copyright holder of any third party material included in this paper, to publish it as part of their paper. The authors confirm that they give permission, or have obtained permission from the copyright holder of this paper, for the publication and distribution of this paper as part of the ICAS proceedings or as individual off-prints from the proceedings.